Quantitative assessment of crystal material and size on the performance of rotating dual head small animal PET scanners using Monte Carlo modeling

Nafise Ghazanfari[1,2] MSc,
Saeed Sarkar[1,2] PhD,
George Loudos[4] PhD,
Mohammad Reza Ay[1,2,3] PhD

1. Department of Medical Physics and Biomedical Engineering,
2. Research Center for Science and Technology in Medicine and
3. Research Institute for Nuclear Medicine, Tehran University of Medical Sciences, Tehran, Iran
4. Department of Medical Instruments Technology, Technological Educational Institute, Athens, Greece

***

Keywords: Small animal PET - Dual head coincidence detector - Geant4 application for tomographic emission - Scintillation material - Inter crystal scattering - Photon penetration

Correspondence address:
Mohammad Reza Ay PhD,
Department of Medical Physics and Biomedical Engineering,
Tehran University of Medical Sciences, Tehran, Iran
Tel/Fax: +98216646638
Email:mohammadreza_ay@tums.ac.ir

Received:
23 December 2011
Accepted Revised:
20 February 2012

Abstract

In this work, among different proposed designs *we have studied* dual-head coincidence detectors (DHC) with pixelated crystals in order to optimize the design of detector systems of small animal PET scanners. Monte Carlo simulations and different detector components and materials, under different imaging conditions and geant4 application for tomographic emission (GATE) were used for all simulations. Crystal length and inter material space on system performance were studied modeling several pixel sizes, ranging from 0.5X0.5mm^2 to 3.0X3.0mm^2 by increment of 0.5mm and using epoxy intermaterial with pitch of 0.1, 0.2 and 0.3mm. Three types of scintillator crystals: bismuth germinate orthosilicate, cerium-doped lutetium orthosilicate and gadolinium orthosilicate were simulated with thicknesses of 10mm and 15mm. For all measurements a point source with the activity of 1MBq was placed at the center of field of view. *The above simulation revealed* that by increasing pixel size and crystal length in scintillator material of a pixelated array, sensitivity can be raised from 1% to 7%. However, spatial resolution becomes worse when pixel size increases from 0.6mm to 2.6mm. In addition, photons mispositioned events decrease from 76% to 45%. Crystal length decrease, significantly reduces the percentage of mispositioned events from 89% to 59%. Moreover increase in crystal length from 10mm to 15mm changes sensitivity from 2% to 6% and spatial resolution from 0.6mm to 3.5mm. *In conclusion*, it was shown that pixel size 2mm with 10mm crystal thickness can provide the best dimensions in order to optimize system performance. These results confirmed the value of GATE Monte Carlo code, as being a useful tool for optimizing nuclear medicine imaging systems performance, for small animal PET studies.

Hell J Nucl Med 2012; 15(1): 33-39 *Published on line: 9 March 2012*

Introduction

Small animal imaging is an important tool for use in non-invasive studies of preclinical animal models [1]. In recent years, research and commercialization of related technologies have increased, due to the flexibility of the detector systems [2-5]. Improvements on these technologies are transferred into scanners, being miniatures of clinical positron emission tomography (PET) systems used for small animal studies [2].

In scintillator based detectors, system performance depends not only on the scintillating materials but also on the scanner design and for that it is essential to optimize the geometry and crystal dimensions of the detecting system [6-8].

Inter crystal scattering (ICS) and photons penetration are also important. Up to now, according to our knowledge, no study has assessed all effective parameters including coincidence events, and using different crystals, in order to evaluate their performance characteristics and their attenuation properties for a dual head PET scanner suitable for small animals imaging.

The present study was focused on the pixelated dual head systems, which are cost-effective and can satisfy the requirements of basic PET studies [9]. By a Monte Carlo (MC) approach, the geant4 application for tomographic emission (GATE) simulation package was utilized in order to study the effect of different scintillator crystal materials and dimensions [10]. The accuracy of GATE in design optimization and performance prediction, of nuclear medicine imaging systems has also been studied.

Materials and methods

Simulation code

The GATE simulation package is based on the well validated Geant4 libraries, is widely used in nuclear medicine [1-11] and offers the possibility of describing complex scanner geometries, in the wide range of tomographic systems. Furthermore, GATE is a proper tool

in the evaluation of new imaging devices [12] and allows for precisely modeling physics studies and for studying time dependent phenomena such as source or detectors movement or source decay kinetics [13-14].We have also tracked the history of each annihilated photon along its trajectory, including the locations of scattering interactions, thus enabling detailed investigation of all system parameters.

GATE modeling of the scanners

The first step in GATE simulation is the definition of geometry. For scanners modeling, we took advantage of block design technology. Each block consists of a crystal array, which consists of grouped crystals in a matrix and forms a pixelated scintillator array, coupled to a position-sensitive photomultiplier (PS-PMT) as shown in Figure 1.

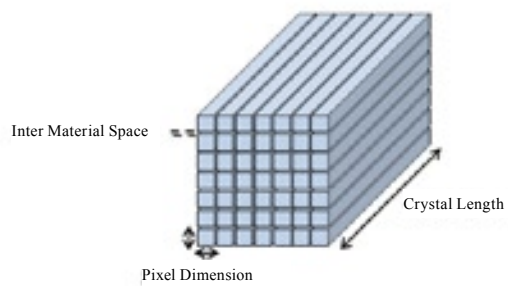

Figure 1. Graphical illustration of designed pixelated array.

In this design, coincidences are only allowed between the two opposite detector blocks and without rotation of the detecting heads it is not possible to attain complete projections from the entire field of view (FOV). Due to the unconventionally defined geometry, only ASCII and ROOT (the data output formats in GATE) were used for the post-processing analysis.

Since achievement of the highest performance significantly depends on different parameters such as crystal type, crystal size and intermaterial crystal dimensions, which are essential to specify. In order to assess the influence of crystal dimensions on the aforementioned parameters, several pixel sizes ranging between 0.5X0.5mm^2 and 3X3mm^2 with step size of 0.5mm were considered. Simulations were carried out by using 0.1, 0.2 and 0.3mm of epoxy (a common industrial material for designing detectors) as intermaterial space to assess the effect of these parameters for difference crystal pixel size. The crystal material was bismuth germinate orthosilicate (BGO), or cerium-doped lutetium orthosilicate (LSO) or gadolinium orthosilicate (GSO). Table 1 summarizes the most important specification of the system characteristics for the scanner used in this study.

Table 1. *Characteristics and geometrical features of simulated systems*

Characteristics	Geometrical features
Detector ring diameter (mm)	100
Number of detectors module	2
Crystal material	BGO/LSO/GSO
Crystal pixel size (mm)	From 0.5X0.5 to 3X3(step 0.5)
Crystal length (mm)	10& 15
Total effective area of scintillator (mm^2)	50±0.7
Inter crystal material	Epoxy
Inter crystal space (mm)	0.1, 0.2, 0.3

BGO: germanate orthosilicate, LSO: cerium-doped lutetium orthosilicate, GSO: gadolinium orthosilicate

The next definition stage in MC simulation modeling is to assign system electronics, which in GATE simulated data acquisition system are identical with the scanner's detection electronics system. The digitizer chain begins with a module called Adder. The Adder module translates the energy deposed of hits from a photon or particle interaction within a crystal, into a pulse. Following the readout module, which is related to a block of crystal, all pulses are gathered as a group and presented as one pulse [12]. Then, a Blurring module is used to apply efficiency factors, using the assumption of 25% energy resolution at the reference of 511keV peak on the output pulses of the readout. Energy window discriminator is applied by setting a lower and upper threshold between the 300-650keV. The dead time module is applied on the crystal block (300ns). So, the coincidence sorter module applies a coincidence window width of 6sec for generating coincidence events. The implemented digitizer chain used in the simulation is shown in Figure 2.

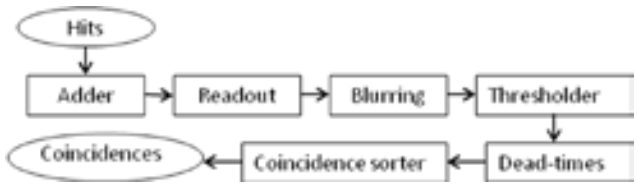

Figure 2. The implemented digitizer chain in GATE simulation.

Performance assessment of scanners

Sensitivity: After accurate modeling of the system in GATE conditions, a point source with the activity of 1MBq was placed at the center of FOV for sensitivity measurements. The simulations were performed using six different values for pixel dimensions and two different crystal lengths for three different crystal materials. Sensitivity was expressed as percentage of the total coincidences per activity (kcps/MBq) (represented as Equation 1). It was not possible to use the same effective area for all pixel dimensions in order to study its role on the sensitivity of the scanners. For this reason, we propose a factor named normalized sensitivity (NS) by dividing the achieved sensitivity of the effective area by the specific pixel affective area (Equation 2).

$$Sensitivity=(Total\ coincidence\ rate\ (cps)/Activity\ (Bq))X100 \quad (1)$$

$$NS=Sensitivity/Affective\ area \quad (2)$$

Intercrystal scattering and penetration: Penetration effects happen whenever an incident photon without any interaction passes through the crystal which is hit to it and then detected in the other position in the wrong place of detector (in pixilated scintillator). It could cause an error which is called parallax error. It significantly influenced by the crystal materials of the detectors and photon incident energies. Whereas, the basic operation in PET systems is accor-

ding to detecting photons with energy of 511keV, this error will be significantly substantial for this kind system. On the other part, Inter crystal scattering phenomena happen for both, non-perpendicular and perpendicular photons that abandoned the interacted crystal after one or more Compton scattering interaction and detected in other crystals. These two phenomena could cause mispositioning in the detection of right place of LOR, because some photons detected in the crystals not correspond to the original position of photons emission. In Figure 3 the inter crystal scattering and photon penetration are presented. For classification of the data which are stored in the ASCII output of the GATE, we used a post-processing algorithm applied on position of the registered LOR, to mark the number of intradetector events. For primary grading events, all random coincidences and scattered photons, before reaching the detector, were eliminated from the output data of simulation**.** Other post processings were conducted on the coincidences that had reached detectors, in order to characterize random coincidences events. The rest of events were marked as true coincidences. The result of post processing was to identify mispositioned events caused by ICS or ICS penetration.

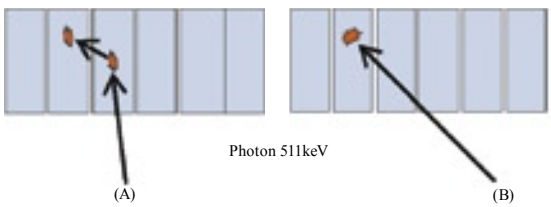

Figure 3. Illustration of (A) inter crystal scattering and (B) photon penetration.

For each simulation, true coincidence events were evaluated according to the position of LOR registration. Two detection elements (pixels) were used in the registration of LOR. Every two pixels of the detector were defined as: a tube of response (TOR) which connected the two pixels to each other instead of a LOR. So, by using this software the deviation of mispositioned LOR from the known position of the source was calculated. If the examined position of the point source was in the TOR the event was considered as a purely true coincidence; if not, as a mispositioned coincidence. Furthermore, GATE has the possibility of registration of Compton events. Related to the destination of each single photon in a coincidence event, mispositioned events were classified and assembled into three associated groups. When one or two single photons underwent penetration it was considered as Group 1. The possibility of registration of Compton events is available in the GATE, so, the mispositioned were classified and assembled into three associated groups that were related to condition happen for each single photon in a coincidence event, if two singles or one of them just underwent penetration it was considered as Group 1. In fact, Group 1 included mispositioned events, which suffered penetration and were free of ICS. If one of the two single events had undergone ICS or penetration and the other did not, it was considered as Group 2. If both single events underwent ICS or penetration they were categorized as Group 3. Figure 4 illustrates the grouping of coincidence events, in order to categorize and distinguish LOR, as purely true coincidences and LOR as mispositioned.

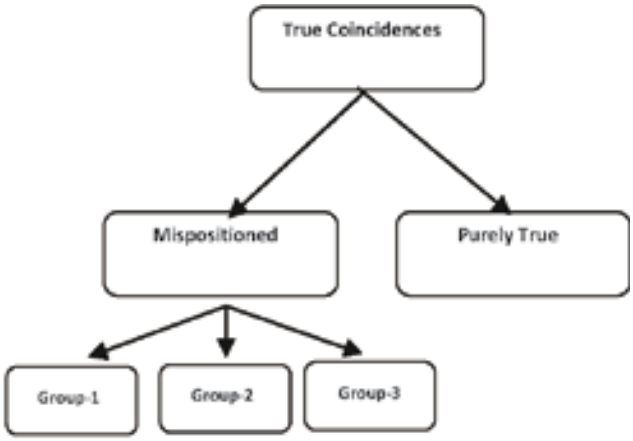

Figure 4. The algorithm for classification of coincidences.

*Spatial resolution:*To determine spatial resolution, the same source described in the previous step was followed. Spatial resolution was measured by considering a point source at the center of FOV. In DHC geometry it was not possible to attain complete projections from the entire FOV, so by implementing rotation with the speed of 3 degrees/sec, all projections were obtained[15].

In order to determine spatial resolution, defining sonogram was an important step. For typical scanners geometry, an in-house prepared software was accomplished to rebin the collected data from three-dimensional (3D) into two dimensional (2D). After each data acquisition, rebinning applied by exploiting single-slice rebinning (SSRB) algorithm.

On the other hand, in the defined sinogram, bin size had a direct effect on the calculation of full width half maximum (FWHM). In consideration of an appropriate sinogram, different dimensions of bins with respect to each pixel size were utilized. In each sinogram a Gaussian curve was fitted on a line generated from projections to derive FWHM [16].

Results

Sensitivity: Figure 5 illustrates a comparison between sensitivity of three different crystal materials as a function of crystal pixel size for discrepant inter material space of epoxy with dimensions 0.1, 0.2 and 0.3mm. By increasing crystal pixel dimestions, sensitivity increases, but extending space between crystal dimension has a significant degrading impact on coincidence registration and the percentage of sensitiviy for differnt designs of PET scanners. It is not possible to define a "half-crystal" in GATE, so for various pixel dimensions the effective area changes. Hence, for making comparable results the concept of NS was proposed. As it is also shown in Figure 5, this parameter has a similar trend for all assessments. By increasing pixel dimensions, sensitivity increased and by increasing inter material space, sensitivity decreased.

Another parameter which induces the percentage of registered coincidence and the sensitivity of the system is crystal length. All aforementioned dimensions and materials were assessed by using an inter material distance equal to 0.2mm and a crystal length of 15mm.The achieved results are represented in Table 2.

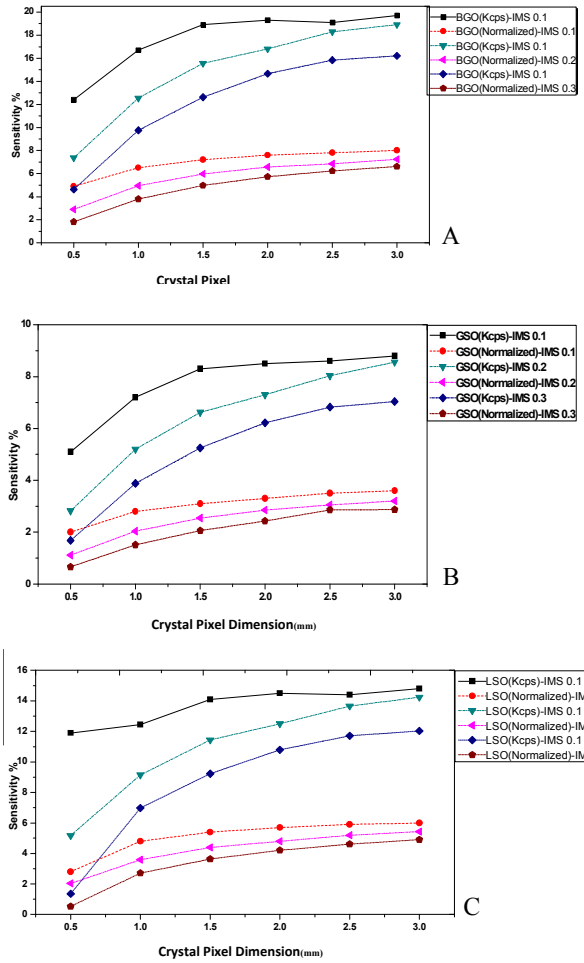

Figure 5. Simulated sensitivity for different crystal pixel and inter material space size and factor of normalized sensitivity (NS), **A.** BGO, **B.** GSO and **C.** LSO.

Inter crystal scattering and penetration: Various dimensions with different crystal materials were considered in order to quantify the percentage of mispositioned events by the percentage of ICS and by penetration. Figures 6a, b and c demonstrate the proportion of mispositioned events (ICS–P coincidences) as a deduction of true coincidences and the number of events, which were registered without any Compton inter-

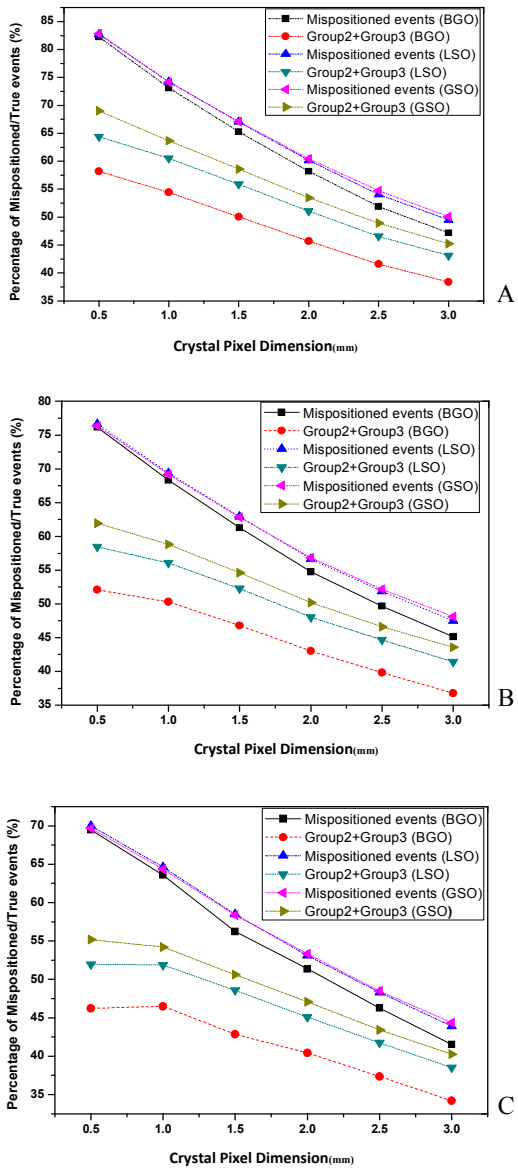

Figure 6. Percentage relative ratio of mispositioned events to true events for different crystal materials as function of crystal size. **A.** inter material space 0.1, **B.** inter material space 0.2 and **C.** inter material space 0.3.

Table 2. *Sensitivity for different crystal dimensions as function of crystal length*

Crystal material	Sensitivity \ Crystal pixel size in mm	3.0	2.5	2.0	1.5	1.0	0.5
BGO	kcps/MBq	14.42	14.05	13.18	12.4	10.58	6.83
	Normalized to Effective area (mm^2)	5.49	5.44	5.15	4.79	4.16	2.7
LSO	kcps/MBq	11.97	11.65	10.85	10.15	8.43	5.21
	Normalized to Effective area (mm^2)	4.57	4.43	4.32	3.91	3.32	2.05
GSO	kcps/MBq	8.02	7.89	7.25	6.69	5.41	3.11
	Normalized to Effective area (mm^2)	3.12	3	2.83	2.57	2.13	1.22

kcps: kilo counts per second

Table 3. *Variation in the percentage of misposition in comparison of crystal dimensions as a function of intermaterial space*

Crystal material	Inter material space \ Crystal pixel size in mm	3.0	2.5	2.0	1.5	1.0	0.5
BGO	0.1-0.2	2.02	2.21	3.43	4.02	4.80	6.10
	0.2-0.3	3.59	3.39	3.40	5.04	4.71	6.68
	0.1-0.3	5.62	5.60	6.83	9.06	9.51	12.78
LSO	0.1-0.2	2.00	2.16	3.51	4.11	4.85	6.09
	0.2-0.3	3.58	3.55	3.50	4.43	4.74	6.65
	0.1-0.3	5.58	5.72	7.02	8.55	9.59	12.74
GSO	0.1-0.2	1.97	2.54	3.59	4.26	4.97	6.47
	0.2-0.3	3.75	3.66	3.48	4.48	4.82	6.70
	0.1-0.3	5.72	6.21	7.08	8.74	9.80	13.17

Table 4. *Variations in the percentage of misposition as a function of crystal thickness*

Crystal material \ Crystal pixel size in mm	3.0	2.5	2.0	1.5	1.0	0.5
BGO	11.36	11.38	11.04	10.30	10.35	7.491
LSO	10.95	11.44	11.09	10.21	9.14	7.66
GSO	11.86	11.93	11.41	10.62	9.56	7.73

actions in the detector (Group 1) or without Compton effects for none of the single photons (Group 2) or with at least one of the single coincidence photons affected by the Compton scattering (Group 3). Purely true coincidences were grouped as a function of pixel element sizes for the BGO, LSO, and the GSO crystal, respectively, in order to study the impact of crystal material on the simulation output. It can be seen in Figure 6 that each of the pixel dimensions of 0.5mm and 1.0mm have the same trend in registration of mispositioned events with the inter material distance of 0.3mm. Pixel dimensions of 1.5mm and 2.0mm and furthermore crystal dimensions of 2.5mm and 3.0mm can be assorted in similar groups. Figure 6 also illustrates the behavior of (ICS–P coincidences) and coincidence events related to the LOR which are registered on incorrect position for BGO, LSO and GSO. The results for data comparison as a fuction of different inter material thickness are given in Table 3. Here, the methods used for estimating the effect of crystal length on the percentage of scanners' sensitivity were exploited to qualify the effect of these parameters on the registration of mispositioned events. Table 4 represents the quntified results for these parameters.

Spatial resolution: Spatial resolution of the point spread fuction was also measured. The point spread function was determind by fitting a Gaussian curve on a profile generated from the projections. In Figures 7a, b, c the simulated spatial resolution of the systems with BGO, LSO and GSO, is illustrated. By increasing pixel elements, FWHM decreases in the same way as the outcome of registration of the mispositioned events. The crystal dimensions were divided into three groups and each two consecutive pixel sizes were categorized in the same group because they showed the same behavior. In addition to assessing crystal pixel size, the effect of crystal length on FWHM was evaluated. The results are demonstrated in the Figure 8 for two crystal lengths of 10mm and 15mm and for different crystal materials (see also Fig. 9).

It was shown that by increasing pixel dimensions, NS will be increased between 1% and 7%. The minimum amount of 1% corresponds to pixel size 0.5X0.5mm^2 with inter material

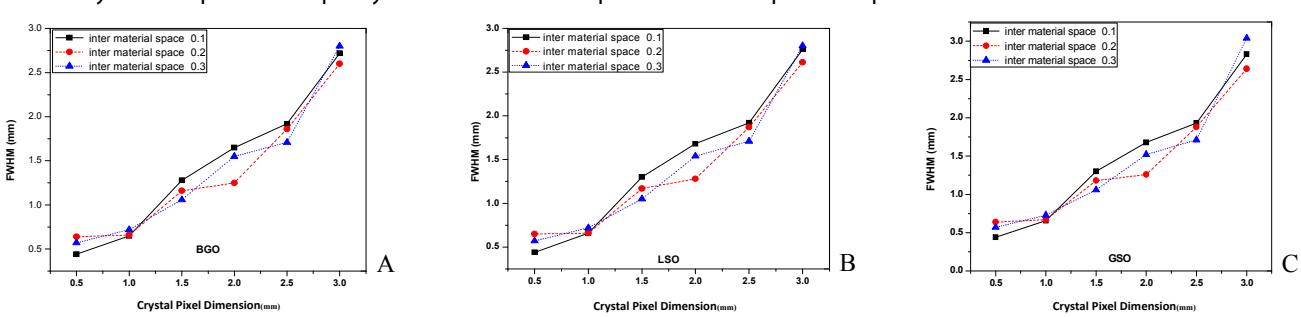

Figure 7. Spatial resolution as a function of pixel size- intermaterial space-crystal material. A. BGO, B. LSO, C. GSO.

space of 0.3mm and the maximum amount of 7% is related to NS of pixel dimensions 3.0X3.0mm^2 by considering inter material spce 0.1mm.

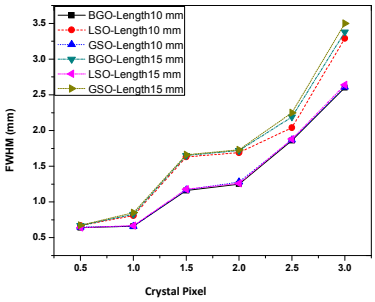

Figure 8. Spatial resolution as a function of crystal length by scale up crystal dimensions.

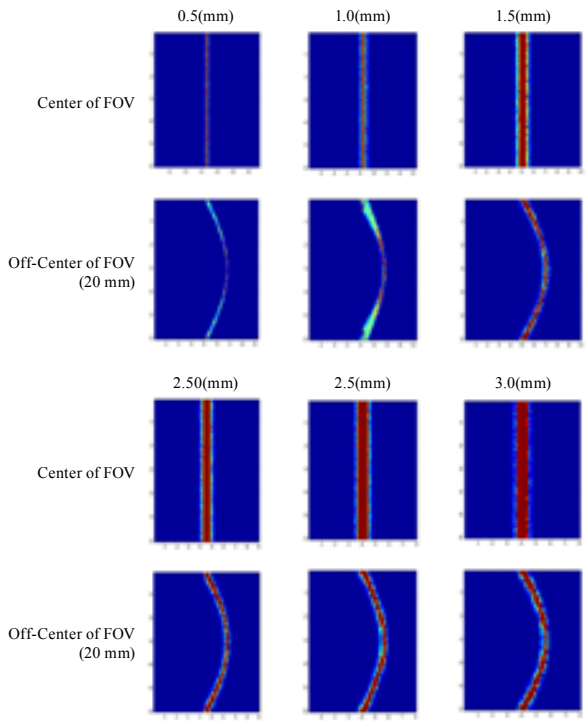

Figure 9. The illustration of a point source at the center and 20mm of center of FOV.

Discussion

To the best of our knowledge, all published studies for assessing limitation of inter crystal scattering (ICS) and penetration for the detection of the right position of line of response (LOR), assume that photon have single energies of 511keV instead of coincidence events [17-20]. It should also be noted that considering a single-photon study instead of coincidences does not provide useful information for the generation of the system matrix that can be used for accurate image reconstruction [3]. Efforts have been made to quantify ICS and parallax error in coincidence mode, which can be used for generation of an accurate system matrix. Whereas, statistical image reconstruction methods are based on system matrix and this matrix is formed according to LOR. Considering a single-photon study instead of coincidences does not provide adequate and correct details, so, exploiting photons as coincidences for organizing LOR in system matrix has a key role in image reconstruction [19].

It is apparent in Figure 6, that by increasing the crystal dimensions, the percentage of mispositioned events is significantlly increased. This is due to the fact that only for small dimensions, the probability of entering photon to the other pixels over increscent of oblique entrance angle intensifies. It can also be deduced that crystal dimensions are supposed to be categorized into three pixel dimnesions (small, medium and large pixel size). Future work in this area will include the incorporation of other attributes of crystals, such as crystal timing features and optical properties.

As it is obvious from Figure 7a, b and c, the intermaterial space plays a critical role on the FWHM. For small pixel dimensions (0.5X0.5mm^2 and 1.0X1.0mm^2) among all proposed intermaterial spaces (0.1mm, 0.2mm and 0.3mm), 0.1mm offers better FWHM altough it may be assumed that 0.3mm and 0.2mm could provide less number of mispositioned coincidences because the probability of entering photons in the other pixels decreases. Since if pixel dimensions and the space between them had more or less the same order, we could not achieve the suitable FWHM. For medium pixel size (1.5X1.5mm^2 and 2.0X2.0mm^2), the intermaterial space of 0.2mm could provide proper FWHM in respect to others. Finally, for large pixel size (2.5X2.5mm^2 and 3.0X3.0mm^2), the 0.2mm space seems to provide better results and the 0.3mm can be acceptable.

The quantitative trend of mispositioned events (ICS–P coincidences) for LSO and GSO more or less is the same; but for BGO, the number of mispositioned events for the registrations applied is lower especially for the extended crystal pixel size (Fig. 6). We should note the high stopping power of the BGO for photons with 511keV energy, due to its atomic number. Morever, not only crystal dimensions but also inter material space influences percentage of registered mispositioned events. In addition, systems with inter material space of 0.1mm were experience more mispositioned events.

As it can be observed from the results obtained from both crystal dimensions and the intermaterial space between two pixels havenegative impact on the FWHM (Fig. 7).

From Table 3, it can be shown that by changing inter material space for different designs of scanners the percentage of mispositioned coincidences changes between 2% to 6%. As it is presented in the Table 3, a steady increase in the percentage of mispositioning variation exists in comparison with the crystal dimensions, as a function of inter material space. The penetration effect is therefore probable for photons entering the crystal at non-perpendicular angles and is intensified when the photon energy is 511keV and the attenuation coefficient (pZ_{eff})of the detector material decreases. As much asthe attenuation coefficient (pZ_{eff})of the chosen crystalsis greater, the percentage of mispostioning events decreases.

In this study we tried to study 3 crystal materials by cinsidering their attenuation properties (aspects) and we did not see any papers which have done the same or even similar and also we considered pixilated crystal which is new in designing detectors.

In conclusion, this study demonstrated by using Monte Carlo detailed analysis that by scaling-up the pixel elements and crystal length, sensitivity of the scanning system increases and also spatial resolution. The above simulation illustrated that BGO based scanners have

higher sensitivity than LSO and GSO scanners and less registration numbers of mispositioned photons, due to their higher attenuation coefficient and ability to absorb more 511keV photons. Proper crystal dimensions were achieved by pixel size of 2mm and crystal thickness 10mm. These results may provide better small animals PET performance.

The authors declare that they have no conflicts of interest.

Bibliography

1. Chatziioannou A. Molecular imaging of small animals with dedicated PET tomographs. *Europ J Nucl Med* 2002; 29: 98-114.
2. Levin CS, Zaidi H. Current trends in preclinical PET system design. *PET Clinics* 2007; 2: 125-60.
3. Panin V, Kehren F, Rothfuss H et al. PET reconstruction with system matrix derived from point source measurements. *IEEE Transact Nucl Sc* 2006; 53: 152-9.
4. Larobina M, Brunetti A, Salvatore M. Small animal PET: a review of commercially available imaging systems. *Curr Med Imag Rev* 2006; 187-92.
5. Meikle SR, Beekman FJ, Rose SE. Complementary molecular imaging technologies: High resolution SPECT, PET and MRI. *Drug Discovery Today: Technologies* 2006; 3: 187-94.
6. Humm JL, Rosenfeld A, Guerra AD. From PET detectors to PET scanners. *EJNM & Mol Imag* 2003; 30: 1574-97.
7. Moses WW. Current trends in scintillator detectors and materials. *Nucl Instrum Methods in Physics Res Section A: Accelerators, Spectrometers, Detectors and Associated Equipment* 2002; 487: 123-8.
8. Rahmim A, Zaidi H. A comparison of BGO, GSO, MLS, LGSO, LYSO and LSO scintillation materials for high-spatial-resolution animal PET detectors: *Nucl Med Comm 2008;* 2835-9.
9. Efthimiou N, Maistros S, Tripolitis X et al. Tomographic evaluation of a dual head PET. *IEEE Imaging Systems and Techniques (IST) International Conference*, Thessaloniki 2010: 27-30.
10. Strul D, Slates R, Dahlbom Ml et al. An improved analytical detector response function model for multilayer small-diameter PET scanners. *Physics in Med Biol* 2003; 48: 979.
11. Agostinelli S, Allison J, Amako K et al. Geant4-a simulation toolkit. *Nucl Instrum Methods in Physics Res-Section A Only* 2003; 506: 250-303.
12. Jan S, Santin G, Strul D et al. GATE: a simulation toolkit for PET and SPECT. *Physics in Med Biol* 2004; 49: 4543.
13. Bao Q, Chatziioannou AF. GATE simulation of a BGO based high sensitivity small animal PET scanner. *Noninvasive Functional Source Imaging of the Brain and Heart and the International Conference on Functional Biomedical Imaging(NFSI-ICFBI), Hangzhou* 2007; 47-50.
14. Buvat I, Lazaro D. Monte Carlo simulations in emission tomography and GATE: An overview. *Nucl Instrum Methods in Physics Res Section A: Accelerators, Spectrometers, Detectors and Associated Equipment* 2006; 323-9.
15. Rechka S, Fontaine R, Lecomte R et al. LabPET inter-crystal scatter study using GATE. *IEEE Nuclear Science Symposium Conference Record (NSS/MIC). Orlando, FL*2009: 3988-94.
16. Shao Y, Cherry SR, Siegel S et al. A study of inter-crystal scatter in small scintillator arrays designed for high resolution PET imaging. *IEEE Transactions on Nuclear Science* 1996; 43: 1938-44.
17. Zeraatkar N, Ay MR, Ghafarian P et al. Monte Carlo-base d evaluation of inter-cryst al scatter and penetration in the PET subsystem of three GE Discover y PET/CT scanners. *Nuclear Instruments and Methods in Physics Research* 2011; 659: 508-14.
18. Lashkari S, Sarkar S, Ay M et al. The Influence of Crystal Material on Intercrystal Scattering and the Parallax Effect in PET Block Detectors: A Monte Carlo Study. *Biomed 2008: IFMBE Proceedings* 2008: 633-6.
19. Fahey FH. Data acquisition in PET imaging. *J Nucl Med Technol* 2002; 30: 39.
20. Ortupo JE, Vaquero JJ, Kontaxakis G et al. Design of a High Resolution Small Animal Octagonal PET Scanner: Preliminary Studies. *Mol Imag Biol* 2003; 5: 120-1.
21. Erlandsson K, Esser P, Strand S et al. 3D reconstruction for a multi-ring PET scanner by single-slice rebinning and axial deconvolution.*Physics in Med Biol* 1994; 39: 619.